DEUTSCHES ELEKTRONEN-SYNCHROTRON DESY

DESY 79/05
January 1979

DEEP INELASTIC QUANTUM CHROMODYNAMIC CHARM LEPTOPRODUCTION

by

M. Glück
Institut für Physik der Universität Mainz

E. Reya
Deutsches Elektronen-Synchrotron DESY, Hamburg

NOTKESTRASSE 85 · 2 HAMBURG 52

To be sure that your preprints are promptly included in the
HIGH ENERGY PHYSICS INDEX ,
send them to the following address (if possible by air mail) :

DESY
Bibliothek
Notkestrasse 85
2 Hamburg 52
Germany

Deep Inelastic Quantum Chromodynamic Charm Leptoproduction

M. Glück

Institut für Physik, Universität Mainz, 6500 Mainz, West Germany

E. Reya

Deutsches Elektronen-Synchrotron DESY, Hamburg

Abstract

The consequences of calculating inclusive charm (or any heavy quark flavor) electroproduction are investigated using a virtual Bethe-Heitler photon-gluon pair creation process. Implications for the light quark sea of the nucleon are studied by comparison with recent μp data in the small x region. Predictions for heavy quarkonium ($J/\psi, \Upsilon$) electroproduction are also given. For example, at $Q^2 = 10\ \text{GeV}^2$ and $x = 0.01$ we find $F_2^{\text{charm}} \simeq 0.08$ and $F_2^{J/\psi} \simeq 0.003$.

Hadronic antiquark (sea) distributions are usually expected to be concentrated in the small x region, in contrast to the broader x distributions of the 'valence' quarks [1]. This is implied by the constituent counting rules [2] as well as in a picture [3,4] where the valence quarks of the hadron radiate gluons which in turn materialize into quark antiquark pairs - the sea. These expectations are vindicated by recent neutrino experiments where it is found [5] that the light antiquark distribution behaves like $(1-x)^{6.7\pm0.5}$ to be contrasted with the valence distribution proportional to $\sqrt{x}(1-x)^{3.5\pm0.5}$ at $x \sim 1$.

So far no similar data are available on the heavy quark (Q) distributions c(x), b(x), ... which are to be considered as sea distributions in ordinary hadrons like the proton or the pion. One usually assumes either [6,7] that due to the heavy mass of these quarks their distribution is zero at some low Q_o^2 and that for $Q^2 > Q_o^2$ these distributions evolve according to the (massless) renormalization group (RG) equations, or [8] that the input distributions are nonzero <u>but</u> very steep in x and that for $Q^2 > Q_o^2$ they again evolve through the RG equations. In both cases the RG equations of a fully massless $SU(4)_{flavor}$ symmetric theory were used. This obviously overestimates the charm development rate and furthermore the input assumption simulates the heavy quark mass only in a rather ad hoc way which probably does <u>not</u> account correctly for the heavy quark mass corrections at $Q^2 \gtrsim 4m_Q^2$. These are probably better reproduced by the lowest order virtual Bethe-Heitler process $\gamma^* g \rightarrow Q\bar{Q}$ which is directly proportional to the gluon (g) content in the nucleon (see fig. 1). Confining our considerations to this amplitude we neglect, in fact, heavy quark production via the electromagnetic current of light quarks q = u, d, s where a $Q\bar{Q}$

pair is produced by a bremsstrahlung gluon as for example shown in fig. 2a. This latter process, although of order α_s^2, is non-negligible since it depends on the valence quark distributions in the proton rather than on the gluons there. However, the leading-log, i.e. dominant piece of these graphs is already contained (see, e.g. fig. 2b) in the RG improved Bethe-Heitler process of fig. 1.

Calculating the contribution of $\gamma^* g \to c\bar{c}$ to F_2 and $F_L = F_2 - 2xF_1$ and convoluting with the RG improved gluon distribution (fig. 1) yields for the <u>total</u> charm production

$$F_{2,L}^{charm}(x,Q^2) = \int_{ax}^{1} \frac{dy}{y}\, y G(y,Q^2)\, f_{2,L}^{\gamma^* g \to c\bar{c}}\left(\frac{x}{y}, Q^2\right) \tag{1}$$

where $a = 1 + 4m_c^2/Q^2$, $Q^2 \equiv -q^2$ and

$$f_2^{\gamma^* g \to c\bar{c}}(z,Q^2) = e_c^2 \frac{\alpha_s(Q^2)}{\pi} \left\{ v\left[4z^2(1-z) - \frac{z}{2} - \frac{2m_c^2}{Q^2} z^2(1-z)\right] + \left[\frac{z}{2} - z^2(1-z) + \frac{2m_c^2}{Q^2} z^2(1-3z) - \frac{4m_c^2}{Q^4} z^3\right] \ln\frac{1+v}{1-v} \right\} \tag{2}$$

$$f_L^{\gamma^* g \to c\bar{c}}(z,Q^2) = e_c^2 \frac{\alpha_s(Q^2)}{\pi} \left\{ 2z^2(1-z)v - \frac{4m_c^2}{Q^2} z^3 \ln\frac{1+v}{1-v} \right\}$$

with the c.m. frame velocity v of one of the heavy quarks given by

$$v^2 = 1 - \frac{4m_c^2}{\hat{s}} = 1 - \frac{4m_c^2 z}{Q^2(1-z)} \tag{3}$$

and $\alpha_s = 12\pi/25\,\ln(Q^2/\Lambda^2)$ with $\Lambda \simeq 0.5$ GeV. Note that the lower limit of integration in eq. (1) as well as $F_{2,L}^{charm}(x \geq \frac{1}{a}, Q^2) \equiv 0$ simply derives from the constraint $v \geq 0$, i.e., $\hat{s} \geq 4m_c^2$. Similar expressions for $f_i^{\gamma^* g \to c\bar{c}}$ as given in eq. (2) have been obtained by Witten [9] and the implications of their n-th moments have been studied in ref. [10].

In neutrino scattering charm is already produced by the weak current in zeroth order, in contrast to electroproduction, via the naive quark-parton process $W^+ s \to c$. In addition, order α_s corrections can be calculated [9,11] stemming from the virtual weak Bethe-Heitler process $W^+ g \to c\bar{s}$. Such calculations, however, appear to be questionable since their results depend now critically on the light s-quark mass chosen, because of the appearance of terms proportional to $\ln(\hat{s} - m_c^2)/m_s^2$. These terms should be absorbed as usual into the RG improved strange quark distribution (s) of the zeroth order $W^+ s \to c$ process.

Similarly, according to the ideas developed in ref. [12], deep inelastic electro- or muoproduction of heavy quarkonia ($J/\psi, \Upsilon, \ldots$) should also be given by

$$F_{2,L}^{J/\psi}(x,Q^2) = \frac{1}{N} \int_{ax}^{bx} \frac{dy}{y}\, y G(y,Q^2)\, f_{2,L}^{\gamma^* g \to c\bar{c}}\left(\frac{x}{y}, Q^2\right) \qquad (4)$$

with $b = 1 + 4m_D^2/Q^2$, which follows from the constraint $\hat{s} \leq 4m_D^2$, i.e., the region of integration extends only up to the threshold of producing "open" heavy quark flavors. The upper limit of integration in eq. (4) obviously implies $F_{2,L}^{J/\psi}(x \geq \frac{1}{b}, Q^2) \equiv 0$. The range of integration as well as the factor 1/N in eq. (4) are due to the duality arguments of ref. [12] which, in

agreement with experiment, indicate that the J/ψ contribution is finally obtained by division through the number of charmonium states N lying in the mass interval $2m_c$ to $2m_D$, i.e. N = 8. Our quantitative results on J/ψ production are expected [12] to be correct within a factor of about 2.

Note that in evaluating the Q^2-dependence of $G(x,Q^2)$ consistency demands application of the $SU(3)_{flavor}$ RG equations, since the heavy quark development is now accounted for by the virtual Bethe-Heitler cross sections in eq. (2). For our actual calculations we have used the fully RG improved gluon distribution of ref. [13] where a "counting rule-like" input distribution

$$xG(x,Q_o^2) = 2.412(1-x)^5 \qquad (5)$$

has been employed at $Q^2 = Q_o^2 = 1.8\ GeV^2$. For the charmed quark mass we have taken $m_c = 1.25$ GeV determined from QCD dispersion sum rules [14]. The resulting charmed quark distributions are shown in figs. 3 and 4. From fig. 3 we observe a very steep and non-negligible (for $x \lesssim 0.01$) contribution: charm production increases rapidly not only for decreasing values of x but also for increasing Q^2. For example, at $Q^2 = 10\ GeV^2$ and $x \simeq 0.01$ we expect the total charm and J/ψ production in F_2 to be about 0.08 and 0.003, respectively, which is about a 20 % contribution to the measured total value of F_2 - effects which should be observable in the forthcoming μ-beam experiments at CERN. This is about a factor of 2 smaller than the RG predictions for massless charmed quarks [6,7]. To show the effects of scaling violations, we have also plotted in fig. 3 the naive parton model

predictions (dashed curves) of eqs. (1) and (4) by using the gluon distribution in eq. (5) with all RG Q^2-dependence turned off. In the very small x-region ($x \leq 0.01$) where, for well known reasons, the full RG improved calculation (solid curves) cannot be applied reliably anymore, the naive parton model predictions should constitute at least a lower bound for the observed charm effects. The scale breaking effects should manifest themselves by observing, say, for $0.01 \lesssim x \lesssim 0.1$ a much steeper increase of charm production in F_2 than expected on grounds of naive parton models. In fig. 4 we show the Q^2-dependence of charm production for various fixed values of x. Total charm production reaches its maximum around $Q^2 = 500$ GeV^2 whereas the maximum of J/Ψ production lies around $Q^2 \simeq 10\text{-}20$ GeV^2. Increasing Q^2 beyond these values, the production of heavy quark flavors decreases rapidly due to the vanishing Bethe-Heitler cross section for large $\hat{s} \sim Q^2$. Some of these qualitative effects stemming from the lowest order Bethe-Heitler calculation may be altered for $Q^2 \gg 4m_c^2$ where higher order logs, i.e. RG-like corrections become important.

From figs. 3 and 4 it is clear that at low values of x ($\simeq 0.01$) and Q^2 ($\simeq 2$ GeV^2) the total charm production in F_2^{charm} is negligibly small. Thus, mainly light SU(3) sea-quarks have to account for the rather large value of $F_2^{\mu p}(x \simeq 0,\ Q^2 \simeq 2\ \text{GeV}^2) \simeq 0.4$ recently measured at Fermilab [15]. The large sea distributions suggested by this measurement can be reconciled with $F_2^{\nu N}$ by taking into account SU(3) broken sea distributions $\bar{u}(x) = \bar{d}(x) \simeq \frac{1}{2}s(x)$, as suggested by recent neutrino experiments [5,16]. From [17] $F_2^{\nu N}(x \simeq 0) = 4x\bar{u} \simeq 1$ below charm threshold ($\theta_c = 0$), and [5] $F_2^{\nu N}(x \simeq 0) = 4x\bar{u} + 2xs \simeq 1.2$ above charm threshold we obtain

$$x\bar{u} = x\bar{d} \simeq \frac{1}{4}(1-x)^7, \quad xs = x\bar{s} \simeq \frac{1}{8}(1-x)^7 \tag{6}$$

at $Q^2 \simeq$ 1-4 GeV^2 and where we have used a $(1-x)^7$ dependence [2,5] for light quark distributions. The sea in eq. (6) is larger than the "standard" value [1,6,13] assumed for the SU(3) symmetric sea which yields also values too low for the Drell-Yan cross section [18]. Thus eq. (6) will help to close the gap between theoretical predictions for dimuon production cross sections and the observed ones [19]. To illustrate the size of F_2^{charm} when compared with actual data, we show in fig. 5 the predictions of eq. (1) on top of $F_2^{\mu p}(x \simeq 0.01) = (\frac{4}{9}xu_v + \frac{1}{9}xd_v) + (\frac{10}{9}x\bar{u} + \frac{2}{9}xs) = (0.08) + (0.285) = 0.365$, where we used eq. (6) and the standard valence contribution at $Q^2 \simeq 2$ GeV^2 of refs. [6,13]. Needless to say that, because of scaling violations, this naive estimate of 0.365 will be an underestimate for $F_2^{\mu p}(x \simeq 0)$ for $Q^2 > 2$ GeV^2. We leave these scale breaking effects in valence and light sea distributions to a future detailed analysis. For $x < 0.01$ we also show in fig. 5 the prediction corresponding to the naive, Q^2-independent gluon distribution of eq. (5) (long-dashed curves) which should yield at least a lower bound for the observed charm effects.

It seems therefore appropriate to conclude that the amount of charm produced by the process $\gamma^* g \rightarrow c\bar{c}$ accounts for <u>all</u> the charm component of $F_2(x,Q^2)$ presently observed. This means, in the language of RG improved Q^2 dependent parton distributions that, due to their large mass, c-quarks in the nucleon can exist only as calculable quantum fluctuations at short distances and that no further "primordial" or initial charm is needed to account for the data at small values of x. A natural test of this conclusion is to check whether eq. (1) indeed accounts for all excess

dimuons and trimuons observed in high energy μp scattering experiments [20]. Because of the cuts on the muon energies and angles in these experiments, further theoretical assumptions [21,22] must be made before a comparison with these cut data is possible. Specifically, a model about the fragmentation of charmed quarks into charmed mesons must be postulated [23] as well as a model for the weak decays of the charmed mesons. A further ingredient postulated in the analysis of refs. [21,22] is the (x,y) distribution of the electroproduced charmed quarks. This is now uniquely provided for in our analysis by eqs. (1)-(3) and differs from the distributions of refs. [21,22] by having a much steeper x dependence as well as a different Q^2 and threshold behavior.

A detailed analysis of dimuon and trimuon electroproduction data is beyond the scope of this letter and is, as mentioned above, also strongly model dependent. We notice, however, that if charmed quarks are indeed produced by $\gamma^* g \to c\bar{c}$ then their transverse momentum q_T^c relative to the direction of the virtual photon is large ($\sqrt{-q^2} \gtrsim \langle q_T^c \rangle \gtrsim m_c$) which might explain the abundance of secondary muons with large transverse momenta k_T^μ. In refs. [21,22] the charmed quarks had no transverse momentum and the muons acquired their transverse momentum only in the fragmentation and decay processes. The so predicted $\langle k_T^\mu \rangle$ was too small or differently said the predicted rates fell more rapidly with k_T^μ than the data, where the discrepancy showed up already at $k_T^\mu \gtrsim 1.2$ GeV. This might further indicate the relevance of the virtual Bethe-Heitler charm production mechanism.

Finally, in order to demonstrate the smallness of the production of even heavier quarks in $F_{2,L}^{\mu p}$, we plot in fig. 6 the predictions for producing

any $b\bar{b}$ states as well as a bound Υ state. These predictions result from eqs. (1)-(4) with the obvious changes for which we used $m_b = 4.5$ GeV (in agreement with an application of the QCD sum rules [14] to the Υ region), $N = 18$ and instead of $2m_D$ the open bottom threshold was taken to be 10.6 GeV. It is clear from fig. 6 that bottom production, compared to charm production in fig. 3, plays practically a negligible rôle for present μ-beam experiments: Even at $Q^2 = 50$ GeV^2 and $x = 0.01$ F_2^{bottom} is almost two orders of magnitude smaller than F_2^{charm}, and a similar suppression holds for Υ production when compared with J/ψ.

We would like to thank M. Krammer for helpful discussions on heavy quark masses.

References

[1] V. Barger and R.J.N. Phillips, Nucl. Phys. B73 (1974) 269; B102 (1976) 439.

[2] S.J. Brodsky and G.R. Farrar, Phys. Rev. Lett. 31 (1973) 1153; V.A. Matveev, R.M. Muradyan and A.N. Tavkhelidze, Nuovo Cim. Lett. 7 (1973) 719.

[3] G. Parisi and R. Petronzio, Phys. Lett. 62B (1976) 331.

[4] M. Glück and E. Reya, Nucl. Phys. B130 (1977) 76.

[5] CDHS coll.:
K. Kleinknecht, lectures held at the CERN School of Physics 1978, Austerlitz-Zeist (Holland), and CERN Yellow Report;

K. Tittel, XIX International Conference on High Energy Physics, Tokyo, 1978;

J.G.H. de Groot et al., QCD Analysis of Charged Current Structure Functions, to be published in Phys. Lett. B; Inclusive Interactions of High-Energy Neutrinos and Antineutrinos in Iron, to be published in Zeitschrift für Physik C.

[6] A.J. Buras and K.J.F. Gaemers, Nucl. Phys. B132 (1978) 249.

[7] I. Hinchliffe and C.H. Llewellyn Smith, Nucl. Phys. B128 (1977) 93.

[8] M. Glück and E. Reya, Phys. Lett. 69B (1977) 77; 72B (1978) 326.

[9] E. Witten, Nucl. Phys. B104 (1976) 445.

[10] M.A. Shifman, A.I. Vainshtein and V.I. Zakharov, Nucl. Phys. B136 (1978) 157.

[11] J. Babcock and D. Sivers, Phys. Rev. D18 (1978) 2301.

[12] M. Glück and E. Reya, Phys. Lett. 79B (1978) 453.

[13] J.F. Owens and E. Reya, Phys. Rev. D17 (1978) 3003.

[14] V.A. Novikov, L.B. Okun', M.A. Shifman, A.I. Vainshtein, M.B. Voloshin and V.I. Zakharov, Phys. Rev. Lett. 38 (1977) 626.

[15] B.A. Gordon et al., Phys. Rev. Lett. 41 (1978) 615.

[16] A. Benvenuti et al., Phys. Rev. Lett. 41 (1978) 1204.

[17] Gargamelle coll.: M. Deden et al., Nucl. Phys. B85 (1975) 269.

[18] M. Glück and E. Reya, Nucl. Phys. B145 (1978) 24.

[19] D.M. Kaplan et al., Phys. Rev. Lett. 40 (1978) 435; J.H. Cobb et al., Phys. Lett. 72B (1977) 273.

[20] C. Chang, K.W. Chen and A. van Ginneken, Phys. Rev. Lett. 39 (1977) 519; K.W. Chen and A. van Ginneken, Phys. Rev. Lett. 40 (1978) 1417; K.W. Chen, Proceedings of the 1977 International Symposium on Lepton and Photon Interactions at High Energies, edited by F. Gutbrod (DESY, Hamburg, 1977), p. 467.

[21] V. Barger and R.J.N. Phillips, Phys. Lett. 65B (1976) 167.

[22] F. Bletzacker, H.T. Nieh and A. Soni, Phys. Rev. Lett. 37 (1976) 1316.

[23] L.M. Sehgal and P. Zerwas, Phys. Rev. Lett. 36 (1976) 399.

Figure Captions

Fig. 1. Bethe-Heitler process for heavy-quark pair $Q\bar{Q}$ production.

Fig. 2. Higher order contribution to $Q\bar{Q}$ production.

Fig. 3. Predictions for total charm and J/ψ production according to eqs. (1)-(4). Solid curves correspond to the full QCD predictions, i.e., using a RG improved Q^2-dependent gluon distribution, whereas the dashed curves refer to the Q^2-independent "naive" gluon distribution of eq. (5).

Fig. 4. Predictions for the Q^2-dependence of charm production for various fixed values of x. The solid curves correspond to those shown in fig. 3.

Fig. 5. Comparison of our QCD predictions for F_2^{charm} with the data of ref. [15]. The short-dashed curves refer to the Q^2-independent base line of $F_2^{\mu p}(x=0.01) = 0.365$ which consists of contributions from light quarks only. Adding to this base line the full QCD prediction of eq. (1) yields the solid curves, while the long-dashed curves represent the corresponding results for the naive Q^2-independent gluon distribution of eq. (5).

Fig. 6. Predictions for total bottom and Υ production where the notation is as in fig. 3.

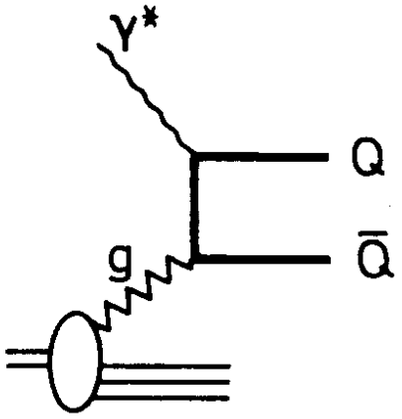

Fig. 1

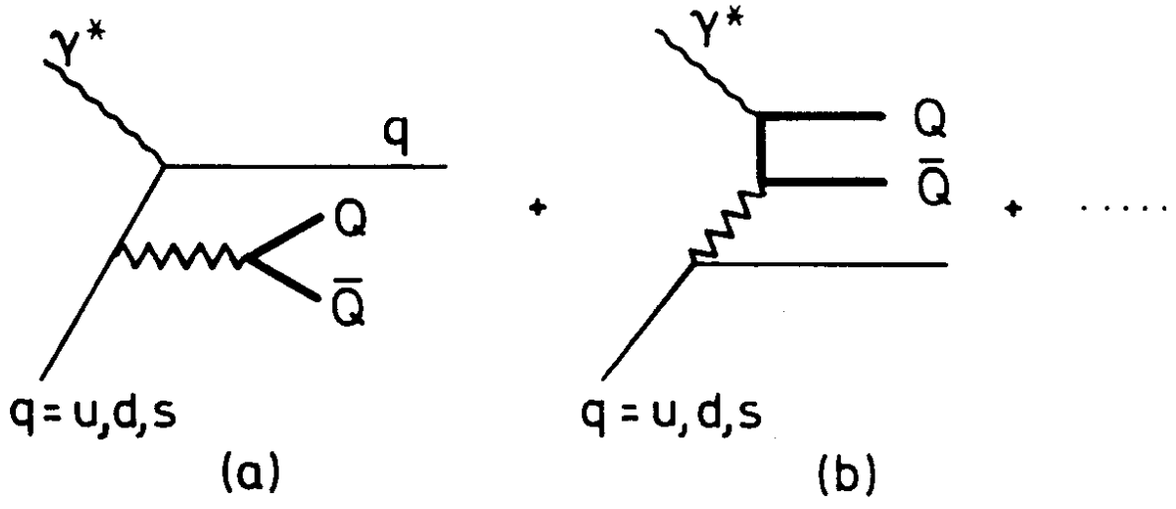

Fig. 2

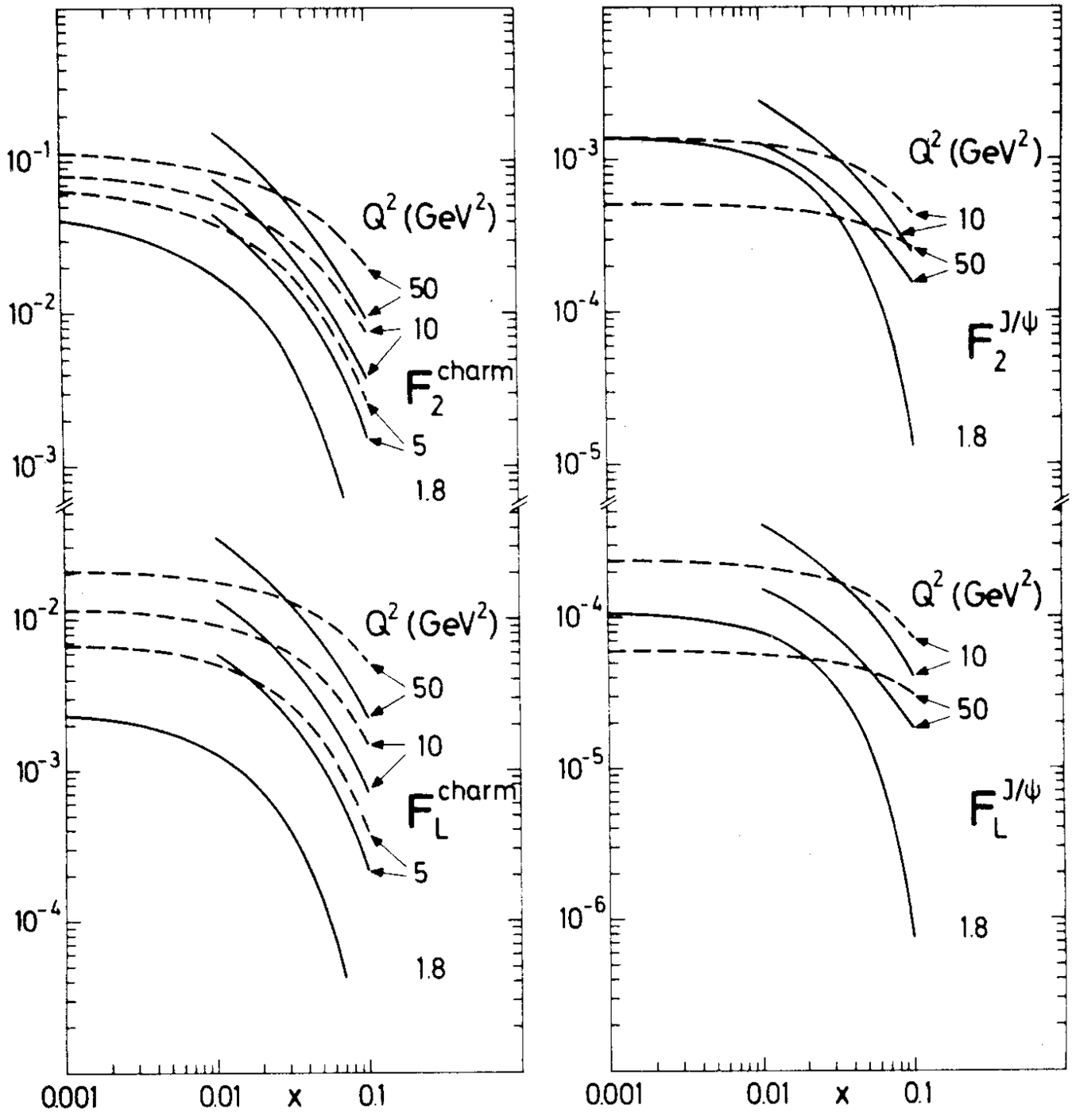
10^{-1}
10^{-2}
10^{-3}
Q^2 (GeV^2)
50
10
F_2^{charm}
5
1.8
10^{-2}
10^{-3}
10^{-4}
Q^2 (GeV^2)
50
10
F_L^{charm}
5
1.8
0.001
0.01
x
0.1
10^{-3}
10^{-4}
10^{-5}
Q^2 (GeV^2)
10
50
$F_2^{J/\psi}$
1.8
10^{-4}
10^{-5}
10^{-6}
Q^2 (GeV^2)
10
50
$F_L^{J/\psi}$
1.8
0.001
0.01
x
0.1

Fig. 3

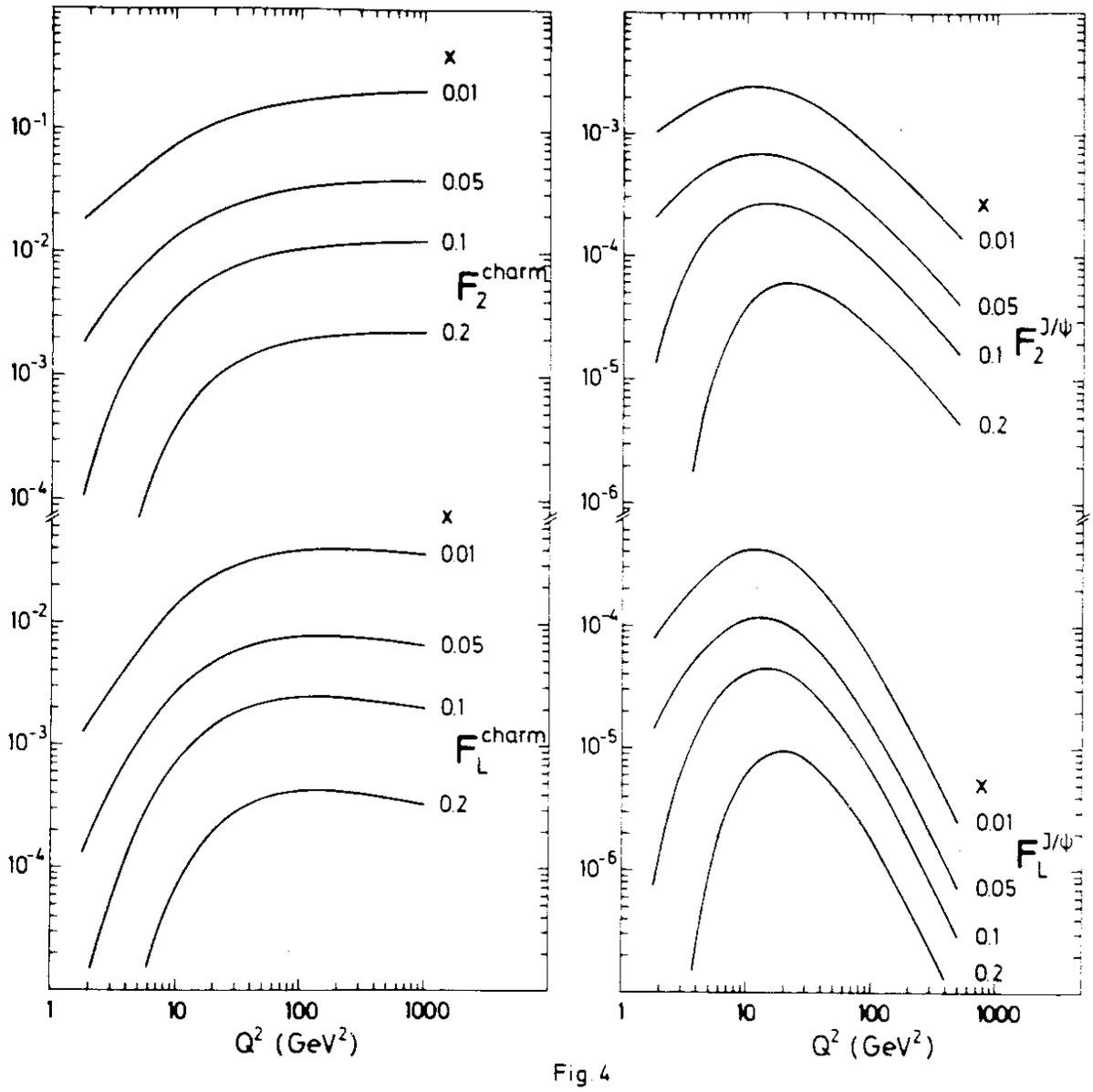
x
0.01
0.05
0.1
0.2
F_2^{charm}
F_L^{charm}
$F_2^{J/\psi}$
$F_L^{J/\psi}$
10^{-1}
10^{-2}
10^{-3}
10^{-4}
10^{-5}
10^{-6}
1
10
100
1000
Q^2 (GeV^2)

Fig. 4

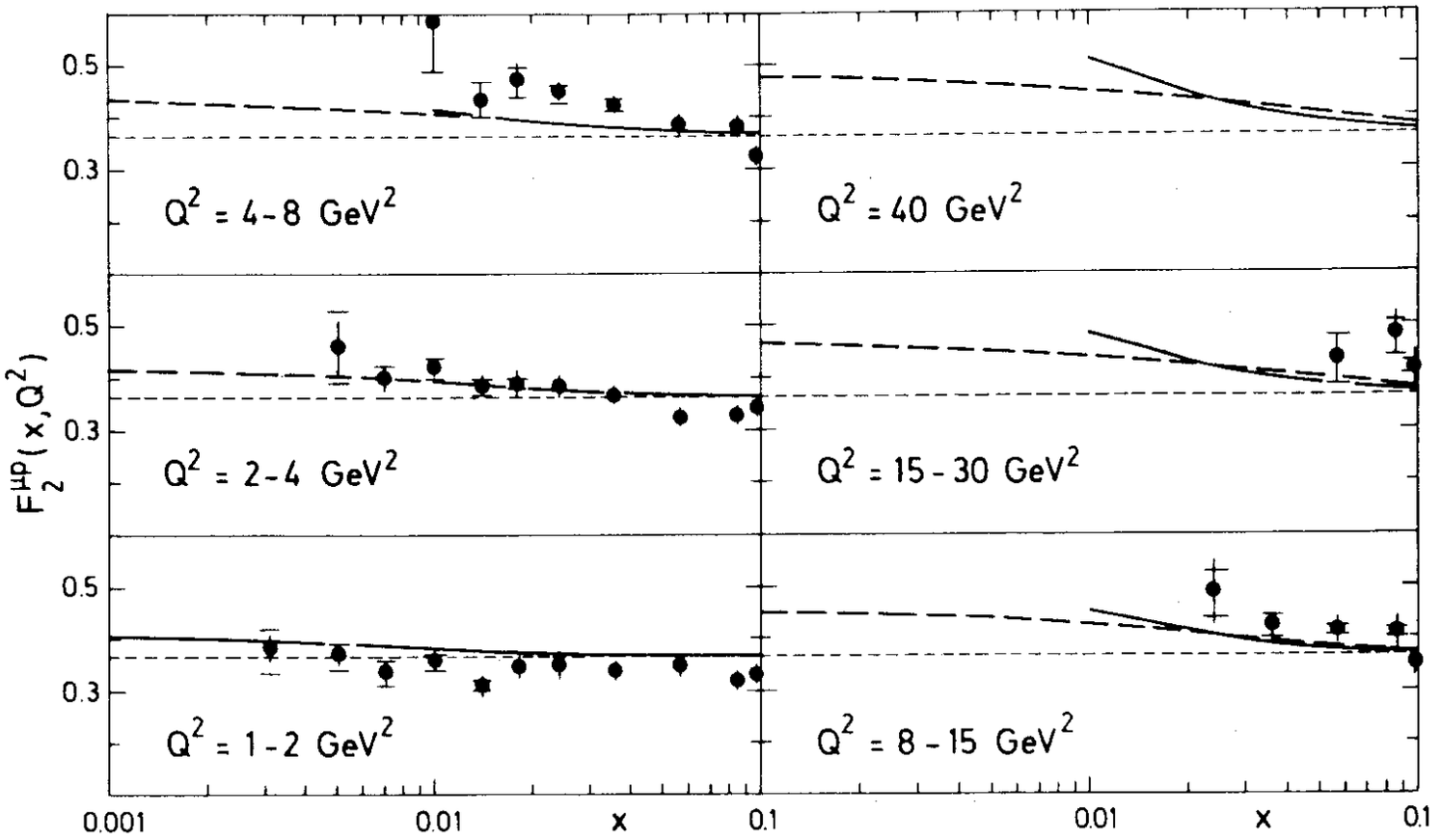
0.5
0.3
Q^2 = 4-8 GeV^2
Q^2 = 40 GeV^2
0.5
0.3
Q^2 = 2-4 GeV^2
Q^2 = 15-30 GeV^2
0.5
0.3
Q^2 = 1-2 GeV^2
Q^2 = 8-15 GeV^2
$F_2^{\mu p}(x,Q^2)$
0.001
0.01
x
0.1
0.01
x
0.1

Fig. 5

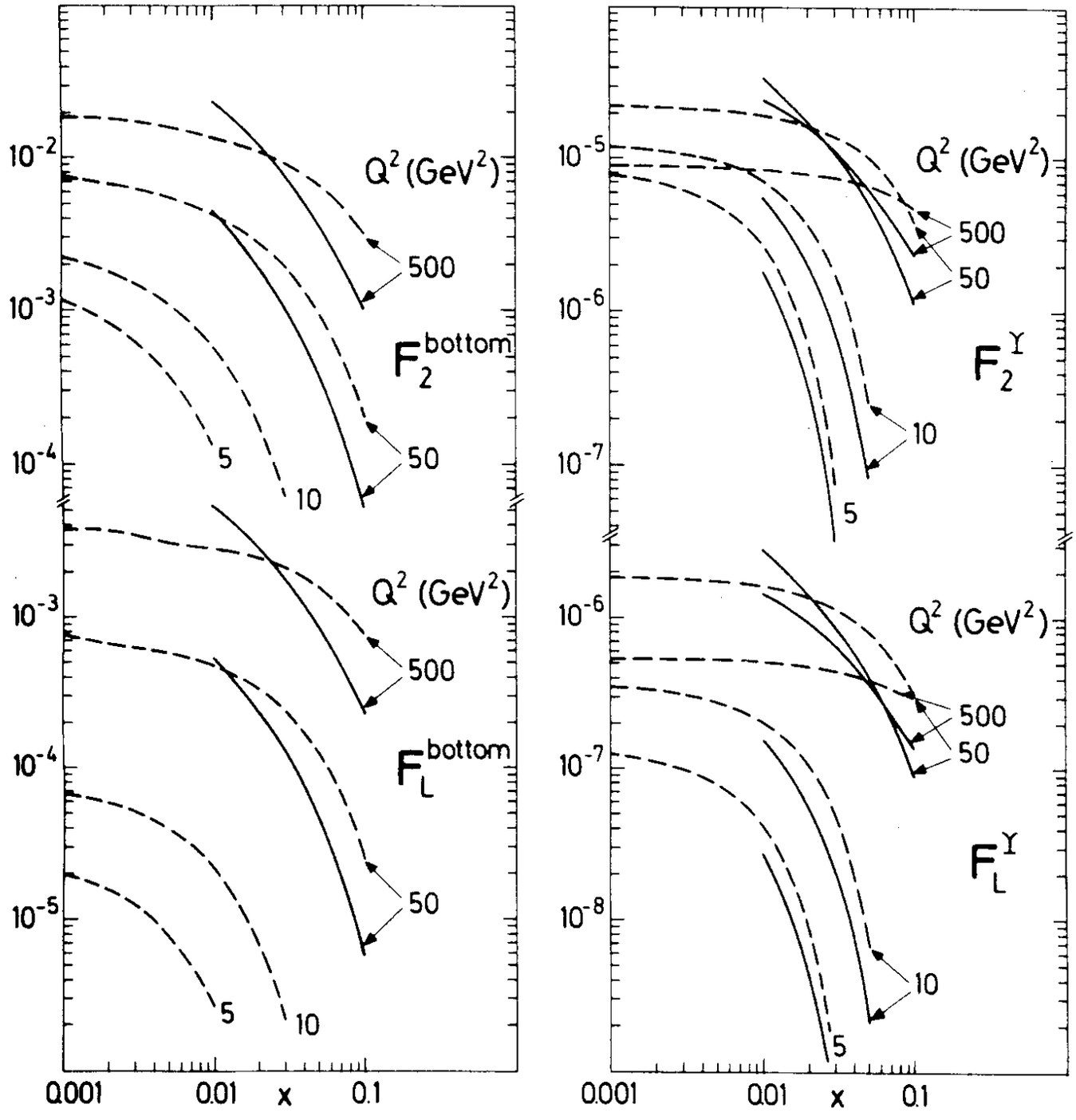
10^{-2}
10^{-3}
10^{-4}
Q^2 (GeV^2)
500
50
F_2^{bottom}
5
10
10^{-3}
10^{-4}
10^{-5}
Q^2 (GeV^2)
500
F_L^{bottom}
50
5
10
0.001
0.01
x
0.1
10^{-5}
10^{-6}
10^{-7}
Q^2 (GeV^2)
500
50
F_2^{Υ}
10
5
10^{-6}
10^{-7}
10^{-8}
Q^2 (GeV^2)
500
50
F_L^{Υ}
10
5
0.001
0.01
x
0.1

Fig. 6